

The use of self-healing technology combined with supplementary cementing materials to mitigate the Alkali-Silica Reaction distress

Diego Jesus de Souza ⁽¹⁾, Leandro Sanchez ⁽²⁾, Alireza Biparva ⁽³⁾, Luan Antunes ⁽⁴⁾

(1) University of Ottawa, Ottawa, Canada, dsouz025@uottawa.ca

(2) University of Ottawa, Ottawa, Canada, Leandro.Sanchez@uottawa.ca

(3) Research and Development Manager, Kryton International Inc, alireza@kryton.com

(4) University of Ottawa, Ottawa, Canada, lantu056@uottawa.ca

Abstract

Alkali-Silica Reaction (ASR) is one of the most harmful distress mechanisms affecting the durability and serviceability of concrete infrastructure worldwide. Over the past decades, several engineers and researchers around the globe have tried to develop preventive measures in the laboratory and in the field to avoid, cease or at least mitigate ASR development rate and damage. It has been shown that ASR-induced expansion and distress could be reduced or delayed by the appropriate use of supplementary cementing materials (SCMs). Moreover, it has been verified that some products, such as crystalline admixtures were able to enhance concrete's healing properties, thus presenting an interesting "physical" solution for durability-related distress due to ASR. In this context, this paper aims to evaluate different concrete mixes presenting two different types of highly reactive aggregates (i.e. Springhill Coarse and Texas fine aggregate), incorporating a wide range of binder compositions (i.e. GU-type cement, silica fume, fly ash, slag and Metakaolin) and using distinct types of chemical admixtures, such as crystalline self-healing and lithium nitrate. The samples were fabricated, exposed to ASR development and monitored over time. Mechanical (i.e. compressive and shear strength, modulus of elasticity and stiffness damage test) and microscopic (damage rating index) techniques were then selected for further analysis on the performance of the distinct mixtures appraised. Comparisons among the results found are made and further discussions and recommendations on the reliability of adopting self-healing products modified with SCMs to suppress ASR are conducted.

Keywords: alkali-silica reaction; the durability of concrete; supplementary cementing materials; self-healing concrete

1. INTRODUCTION

Alkali-Silica Reaction (ASR) is one of the most harmful distress mechanisms affecting the durability and serviceability of concrete infrastructure worldwide. ASR is conventionally defined as a chemical reaction between the alkali hydroxides (i.e. Na⁺, K⁺ and OH⁻) dissolved in the concrete pore solution and some reactive mineral phases containing reactive silica forms present in the aggregates used in the mixture [1–5]. ASR generates a gel that swells in the presence of water, causing volumetric expansion and distress in the affected material. Moreover, ASR *microscopic/macrosopic* distress degree and features depend upon the type (i.e. fine and coarse aggregate) and reactivity of the aggregates used, the amount of alkalis of the concrete, the temperature and relative humidity of the environment along with the exposure and confinement (i.e. reinforcement ratio, etc.) conditions of a given structure/structural member [4,6–11].

Over the years, several approaches and recommendations, including a comprehensive variety of laboratory test procedures, have been developed around the world to assess the potential alkali-reactivity of concrete aggregates and the efficiency of preventive measures (i.e. control of the cement & concrete alkali content, use of supplementary cementing materials - SCMs, etc.) [5,6]. SCMs are known to control ASR expansion mainly by their capacity of reducing the alkalinity of the pore solution by binding alkalis in the hydration products [5], which can be partially justified by the alkali dilution in concrete as a result of the partial replacement of cement by SCMs with lower alkali content [12]. Moreover, it has been reported that the ability of SCMs to bind alkalis seems to be strongly related to the CaO/SiO₂ ratio of the SCMs; i.e. the higher this ratio, the lower its binding capacity [13]. Furthermore,

SCMs with a high (reactive) silica content and a low amount of CaO and alkalis will be the most effective in terms of lowering the pore solution alkalinity and preventing expansion due to ASR [12–16].

1.1 Preventive measures of ASR

The main source of alkalis in concrete is Portland cement (PC). Therefore, the total alkali loading in concrete is obtained through the quantification of the PC alkali content (expressed as $\text{Na}_2\text{O}_{\text{eq}}$) times the PC content of the mixture. Preventive measures, including limiting the alkali content in concrete, may be used to decrease the likelihood of ASR. Amongst those, the use of supplementary cementing materials (SCMs) such as fly ash (FA) [14,16–18], granulated blast-furnace slag (BFS) [12,19,20], silica fume (SF) [21–25] and metakaolin [17,26,27], besides the use of chemical admixtures [27–31] have been widely studied. SCMs are able to control ASR-induced development by reducing the amount of alkalis available in the system, limiting thus their availability to react with the aggregates [1,13,18]. Furthermore, it has been found that the ability of SCMs to bind alkalis seems to be strongly related to the CaO/SiO_2 ratio of the SCMs [13]. SCMs that present a low calcium content and high in silica are more effective in reducing the pore solution alkalinity, and thereby ASR expansion.

Chemically, SCMs are able to dilute the alkalis available from the clinker, decrease the pH of the material by consuming $\text{Ca}(\text{OH})_2$ from the pore solution [1,13,18]. The formation of “new” C-S-H due to SCMs reaction has a greater capacity to entrap alkalis and reduce even more the pH. Furthermore, these materials are able to change concrete microstructure, interfering with the pore size distribution and their interconnectivity among the cementing matrix. This effect reduces the mobility of ions and possibly slows the reaction rate. It also makes the concrete less permeable to external moisture and alkalis [12,13,17,18,32,33]. Some authors revealed that alkali-silica reaction is very similar to pozzolanic reactions preceding to ASR [13,34]. The reactive silica present in finely-ground SCMs reacts rapidly with the alkali hydroxides from the pore solution forming an alkali-silica gel containing small amounts of calcium.

The use of chemical admixtures to reduce ASR-induced expansion and damage or at least to delay the process has been widely adopted since the 1950s. Among several products, lithium compounds have shown a good response in modifying the reaction kinetics as per [27–31]. The first publication referring to this subject is dated from 1951 by McCoy and Caldwell, in which the authors studied over 100 different chemical compounds using ASTM C 227 to control the ASR. The authors concluded that lithium compounds were able to reduce the expansion at 8 weeks of exposure at 38 °C and 100% RH. After some studies to understand how lithium compounds were able to mitigate ASR [30,31], it has been explained that the metastable silica in the aggregates might react with Li-ions modifying the chemical structure of the alkali-silica gel [35,36]. Later, Bulteel et al. [37] and Leemann et al. [38] claimed that Li ions are capable of reducing the solubility and dissolution rate of silica. Finally, three lithium compositions have shown very good results: lithium hydroxide, lithium carbonate and lithium nitrate. The third compound, LiNO_3 among the others has shown better results in controlling ASR. Lithium nitrate stands out for good solubility and slightly alters the pH of the pore solution of the concrete [29–31].

1.2 Improvement of the healing properties of concrete.

It has been verified that some products (i.e. using different types of bacteria, etc.) were able to provide concrete with self-healing properties, which may present a very interesting “physical” solution for durability-related distress in concrete [39–44]. Self-healing is the process through which a material is able to recover its properties, after having suffered some damage coming from a mechanical or durability-based source, with little or no external aid [41–44]. Self-healing in concrete is caused by the following two main mechanisms [39–44]: natural healing (NH) and artificial healing (AH). NH is comprised of the following processes: calcium carbonate (CaCO_3) formation (the so-called carbonation), along with continued hydration upon moisture contact, swelling of cement matrix and sedimentation of debris. Conversely, AH is an engineering-made healing process designed to improve the healing properties of concrete. AH can be further divided into ‘passive’ (requires no human intervention, such as crystalline admixtures) or ‘active’ modes (requires some human aid) [40].

One of the smartest materials used for self-healing applications in concrete is the so-called crystalline admixtures (CA); it is one of the types of permeability-reducing admixtures with hydrophilic nature that reacts easily with water. Authors [42,45] have found that concrete mixtures treated with CA were able to reduce almost 50% of the water penetration depth, enhance the resistance to chloride penetration and recover mechanical properties such as flexural deformation and stiffness. The latter indicates that,

maybe, the use of crystalline admixture might enhance the capacity to mitigate ASR-induced development.

2. SCOPE OF THE WORK

As stated above, a number of techniques, supplementary cementing materials and chemical admixtures have been used in the past aiming to assess and mitigate the initiation and development of ASR in the field. However, there is very few research (if any) on the use of self-healing products combined and or modified with SCMs; hence, forming a binary chemical-physical treatment and leaving room for major developments in this area. The current research aims to evaluate the combination of different types of SCMs and crystalline admixtures for preventing and/or mitigating (i.e. physically, chemically or both) concrete deterioration caused by ASR in its initial, moderate and advanced phases.

3. MATERIALS AND METHODS

3.1 Materials and mixture proportions

Sixteen different concrete mixtures incorporating two distinct highly reactive aggregate types and natures were fabricated. Moreover, four different types of supplementary cementing materials (i.e. blast furnace slag-Sg, fly ash-FA class F, silica fume-SF and metakaolin-MK) and three different admixtures (i.e. lithium nitrate and two commercially available hydrophilic permeability reducing so-called crystalline admixture - CA) were selected for the research. Moreover, it was not used any type of superplasticizer in this research. The coarse aggregates ranged from 5 to 20 mm in size. Non-reactive fine (NF) and coarse (NC) aggregates were also used in combination with two reactive aggregates (SPH and Tx) for concrete manufacturing. Table 3.1 provides information on the different aggregates used in this study. Table 3.2 provides information about the chemical composition of the different binder materials used in this study. All sixteen concrete mixtures were mix-proportioned as per ASTM C 1293 to present the same amount of “reactive aggregates” in volume so that one could compare similar systems (Table 3.3) with different aggregate types and strengths.

Table 3.1: Reactive (R) and non-reactive (NR) aggregates used in the research.

Aggregate		Reactivity	Rock Type	Specific gravity	Absorption (%)	AMBT ^a (%)
Coarse	NC	NR	High-purity fine-grained limestone	2.79	0.42	0.00
	SPH	R	Crushed Greywacke	2.73	0.71	0.33
Fine	NF	NR	Natural derived from granite	2.67	0.82	0.08
	Tx	R	Polymictic sand (granitic, mixed volcanic, quartzite, chert, quartz)	2.63	0.91	0.86

^a Results at 14 days of curing of the accelerated mortar bar testing (ASTM C 1260) carried out on the aggregates selected.

Table 3.2: Chemical composition of the Binder materials.

	Cement	Slag	Fly Ash	SF	MK
CaO	61.93	37.31	10.28	0.62	0.12
SiO ₂	20.1	36.64	56.30	92.85	52.48
Al ₂ O ₃	5.02	11.14	23.26	0.05	44.34
Fe ₂ O ₃	3.80	0.391	3.573	0.12	0.61
SO ₃	4.38	0.366	0.193	0.07	0.03
MgO	2.42	12.15	1.07	0.19	0.08
Na ₂ O _{eq.}	0.91	0.63	2.92	0.52	0.38
LOI	2.91	0.00	0.98	5.05	0.69

Table 3.3: Concrete mixtures cast with different aggregates using the same volumetric amount of reactive aggregates.

Mixture	w/cm = 0.45		Aggregates (kg/m ³)				Admixtures (kg/m ³)		SCMs (kg/m ³)			
	Water (kg/m ³)	Cement (kg/m ³)	NF	Tx	NC	SPH	CA1	CA2	Sg	FA	SF	MK
SPH Control	189	420	836	-	-	938	-	-	-	-	-	-
SPH LTM*	189	420	836	-	-	938	-	-	-	-	-	-
SPH CA1	189	420	836	-	-	938	8	-	-	-	-	-
SPH CA2	189	420	836	-	-	938	-	8	-	-	-	-
SPH Sg	189	210	761	-	-	938	8	-	210	-	-	-
SPH FA	189	294	776	-	-	938	8	-	-	126	-	-
SPH SF	189	376	820	-	-	938	8	-	-	-	44	-
SPH MK	189	357	823	-	-	938	8	-	-	-	-	63
Tx Control	189	420	-	765	1019	-	-	-	-	-	-	-
Tx LTM*	189	420	-	765	1019	-	-	-	-	-	-	-
Tx CA1	189	420	-	765	1019	-	8	-	-	-	-	-
Tx CA2	189	420	-	765	1019	-	-	8	-	-	-	-
Tx Sg	189	210	-	765	1005	-	8	-	210	-	-	-
Tx FA	189	394	-	765	957	-	8	-	-	126	-	-
Tx SF	189	376	-	765	1003	-	8	-	-	-	44	-
Tx MK	189	357	-	765	1006	-	8	-	-	-	-	63

* LTM – Lithium Nitrate (LiNO₃) admixture – the ratio Li/Na was kept constant as 0.74

3.2 Manufacture of the concrete specimens

Thirty-six cylinders, 100 × 200 mm in size, were fabricated for each of the sixteen concrete mixtures in the laboratory. After 24 h, the samples were demoulded and stored in a moist curing room for another 24 h. Then, small holes (5 mm in diameter by 15 mm deep) were drilled at the two flat ends of the samples, in which steel gauge studs were glued in place with a fast-setting cement slurry, for longitudinal expansion measurements. Next, the samples were left to harden over 5 days before the “0” reading was taken; all the samples were finally placed in sealed plastic buckets lined with a damp cloth and stored at 38 °C and 100% R.H.

The cylinders were monitored for length variations at 45 and 90 days of exposure (this research is still being developed until the samples reach 24 months as per CSA A23.2-14A / ASTM C1293). As per ASTM C 1293, the buckets were cooled down to 23 °C for 16 ± 4 h prior to the periodic measurements. Then, the cylinders were wrapped in plastic film and kept under 12 °C to inhibit further AAR deterioration until all shear tests were conducted (due to testing capacity issues).

3.3 Assessment of the ASR development in the concrete

3.3.1 Stiffness Damage Test (SDT)

Three cylinders of each concrete mixture at 90 days of exposure were subjected to five cycles of loading/unloading at a controlled loading rate of 0.10 MPa/s. The SDT procedure was performed following Sanchez et al. publications [3,46,47], i.e. using a loading level corresponding to 40% of the 28-day concrete strength. To characterize all mixtures at 28 days compressive strength, samples were wrapped and placed at 12 °C, since some of the specimens contained highly reactive aggregates and ASTM C 39 method could not be followed as they could develop some ASR. The cylinders were maintained at 12 °C for a 47-day period, according to the maturity concept as per ASTM C 1074.

3.3.2 Damage Rating Index (DRI)

A semi-quantitative petrographic analysis, using the DRI, was performed on one specimen from each concrete mixture at 90 days of exposure, according to the method described by Sanchez [3,9]. The DRI

final number presented in this work is the normalized 100 cm² value obtained over polished concrete specimens.

3.3.3 Compressive Strength Test

Compressive strength was measured through two different approaches with different and specific goals. First, as previously mentioned, the 28 days compressive strength of all mixtures was obtained through the use of the maturity concept as per ASTM C 107 to reach their mechanical capacity values. The second compressive strength measurements were carried out on three cylinders used for stiffness damage testing, with the aim of verifying the compressive strength loss of the material as a function of AAR development. This procedure was adopted and considered valid after Sanchez et al. [3,9] confirmed the largely non-destructive character of the SDT.

3.3.4 Direct Shear Test

The direct shear test was performed according to the method and setup proposed by Barr and Hasso [48] and adapted by De Souza et al. [11]. The same approach considering the maturity concept was used to characterize the “zero” reading for all concrete mixtures at the equivalent 28 days. At 90 days of exposure, three samples of each concrete mixture were selected for analysis; however, differently from the compressive strength tests, the SDT was not performed on the samples prior to the shear test. Before testing, all samples were carefully ground so that a circumferential notch was created [11,48]. The notch depth was adopted as about 20 mm ± 3 mm to ensure a shear-type failure without leaving a too-small area of the sample to be tested.

4. RESULTS AND DISCUSSION

4.1 ASR Kinetics

In this section, ASR expansion kinetics and amplitude results are presented for all sixteen mixtures fabricated in the laboratory, Figure 4.1 presents the average expansion values of each of them. A wide range of expansion kinetics and amplitudes were obtained as a function of the mixtures tested. In general, the mixtures containing the reactive Tx sand presented faster reactivity than those incorporating reactive SPH coarse aggregates. Disregarding the control groups (SPH and Tx - which displayed the greatest expansions), the groups containing only crystalline admixtures presented faster reactivity, reaching 0.10% (CA1) and 0.13% (CA2) for mixtures containing the reactive SPH. Moreover, involving the extremely reactive Tx, it was found that CA1 reaches 0.27% of expansion at 90 days of exposure while CA2 reached 0.30%. Comparing the different aggregates used (SPH and Tx), CA1 and CA2 had a significant variation in ASR reaction kinetics after 45 days of exposure, since the slope of the curve (i.e. expansion rate) significantly decreased for mixtures incorporating the SPH reactive aggregate.

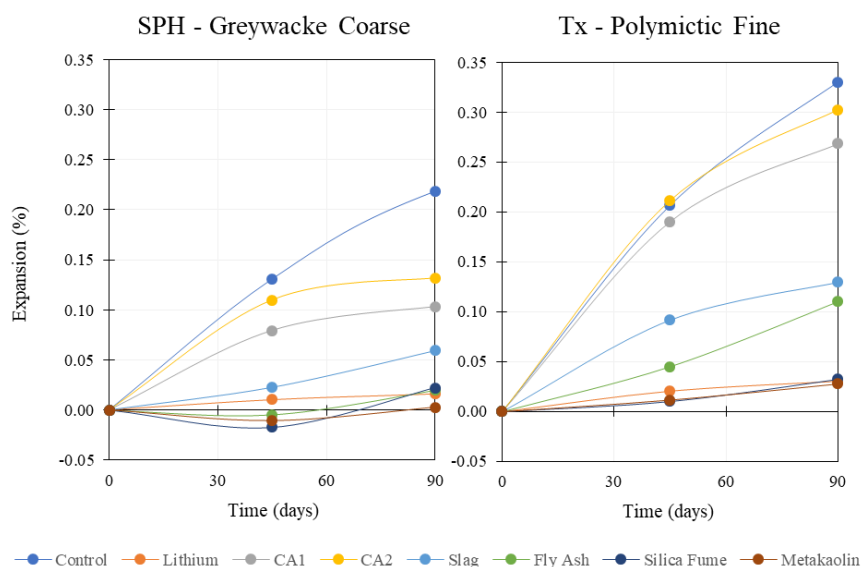


Figure 4.1: Expansion of ASR-affected concrete specimens.

The use of supplementary cementing materials (SCMs) in combination with CA1 was able to significantly change ASR kinetics. The concrete cylinders containing CA1 and Slag at 50% replacement presented 0.06% expansion in the presence of the SPH and 0.13% expansion with the Tx aggregate after 90 days. These values are 73% and 61% lower (SPH and Tx, respectively) than those obtained by the control groups. The samples containing CA1 and 30% of Fly Ash showed 0.02% expansion for SPH and 0.11% expansion with Tx. Shrinkage was often observed at early ages when using high levels of FA, which was seen in SPH samples until 45 days of curing. The same behaviour was also observed for Silica Fume and Metakaolin samples. Both highly reactive SCMs, silica fume and metakaolin have shown a quite efficient behaviour to mitigate ASR. Replacing 10.5% of PC by silica fume decreases the expansion at 90 days of curing to 0.02% and 0.03% (SPH and Tx, respectively). Metakaolin, at least up to date, has displayed the best results, 0.003% and 0.02%, which are 99% and 92% smaller than the control group (for SPH and Tx, respectively).

4.2 Mechanical Properties Assessment

This section evaluates the reductions in modulus of elasticity, shear strength and compressive strength of the various concrete mixtures investigated in this work. The data presented here are the variation ratio of values obtained at each selected “free” expansion level against the values obtained on sound concrete specimens (Figure 4.2). The direct shear test as per De Souza et al. [11] was assessed and the modulus of elasticity was obtained through the SDT method as per Sanchez et al. [3,46,47]. In the plots, 0.0 values mean 0% loss whereas 1.00 values mean 100% reduction. Control samples (Control SPH and Tx) showed the highest mechanical properties losses, followed by the mixtures CA1, CA2 and Slag. Conversely, mixtures containing Silica and Metakaolin yielded the lowest reductions, including the enhancement of some of their properties.

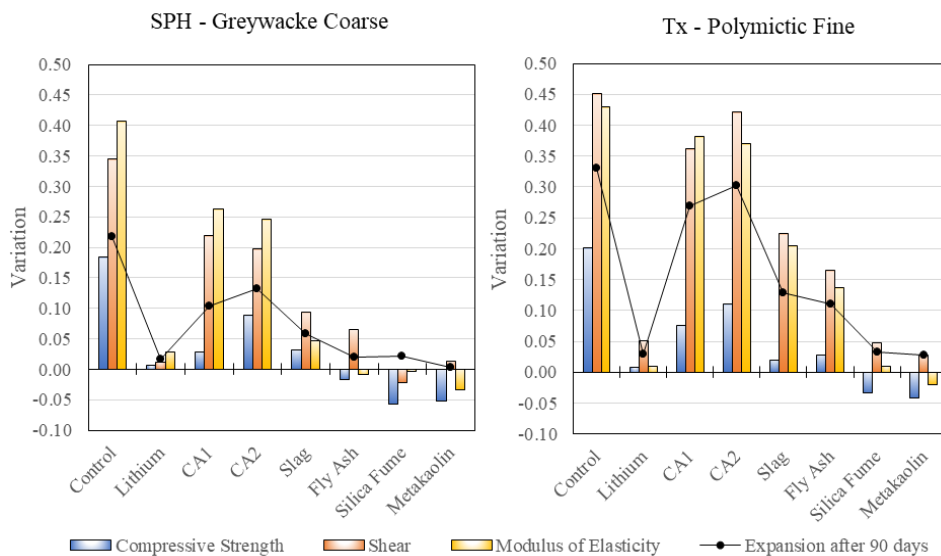


Figure 4.2: Variation ratio among the mechanical properties (Compressive and Shear Strength and Modulus of Elasticity) of ASR-affected concrete specimens.

In general, compressive strength (CS) was found to decrease in a somewhat modest way in comparison with the other mechanical properties tested. For samples with low expansion levels (i.e. Silica Fume, Metakaolin and Fly Ash for SPH aggregate), the compressive strength ranged from -6% to -2% due to the fact that these samples displayed an increase in CS after 90 days of curing. The CS of Lithium samples, also with low expansion levels, were found as 1%, which can be just a small variation on the test procedure and not exactly related to ASR. Otherwise, samples that presented the highest expansion levels (i.e. Control SPH and Tx, CA1 and CA2) up to date, were found to display CS losses of 18% and 20% for Control SPH and Tx, respectively, 9% and 11% for CA2 SPH and Tx, and, 3% and 8% for CA1 SPH and Tx.

The direct shear strength (DSS) results are also evaluated in Figure 4.2. It is observed that all mixtures present a shear strength decrease as a function of ASR induced expansion. The shear reduction is expected to take place due to “shear friction or aggregate interlock loss” caused by ASR-induced

development; the latter seems to be dependent on the aggregate's type (i.e. fine vs coarse aggregate). In samples incorporating Tx aggregate, the shear strength losses were more sensitive, showing similarities with the variations in the modulus of elasticity (ME). Those losses in DSS were even higher than in ME (i.e. Control, Lithium, CA1, CA2, Slag and Fly Ash). The Tx Control samples have shown 45% of DSS loss, which was the higher value obtained. Yet, CA2 and CA1 incorporating Tx have also presented important losses in DSS (42% and 36%, respectively). Direct shear reductions seem to be more important when the matrix starts to have a higher amount of cracks as a result of the higher expansion levels, facilitating the propagation of cracks during the test.

The modulus of elasticity loss plot ranges from -3% (gain in ME, Metakaolin SPH samples) to 43% (Control Tx). In general, the higher the expansion level, the higher the losses in ME. As well known in the literature [8,49–53] for conventional concrete, the modulus of elasticity is largely governed by the mechanical properties of the aggregates, especially the coarse aggregate. Therefore, this phenomenon is likely responsible for the significant decrease in ME of ASR-affected mixtures. As well as for DSS results, ME seemed to be dependent on the aggregate's type (i.e. fine vs coarse aggregate); samples incorporating the highly reactive Tx obtained higher ME losses.

Fig. 2 illustrates the SDI results obtained through the *stiffness damage test* (SDT), in accordance with Sanchez et al. [3,46,47], for all sixteen mixtures tested in this study. SDI values were found to range from about 0.01 (Fly Ash with 0.02% of expansion) to 0.23 (Control with 0.22% of expansion) for SPH reactive Coarse aggregate, and from about 0.02 (Lithium with 0.03% of expansion) to 0.24 (Control and CA2 with 0.33% and 0.30% of expansion, respectively) for Tx reactive fine aggregate. The development of cracks within the aggregate particles and the propagation through the cement paste leads to an extension of inner damage in the affected concrete. Therefore, these cracks while being closed over a compressive and cyclic test, release a significant amount of energy, which results in the fast SDI values rise. Moreover, mixtures incorporating Tx were found to dissipate more energy, since those samples have presented up to the date the highest expansion levels. Additionally, SCMs seems to improve the quality of the ITZ, thus, reducing SDI values, comparing the same expansion levels reached by SCMs sample with those observed by Sanchez et al. [4] and obtained with non-SCMs systems.

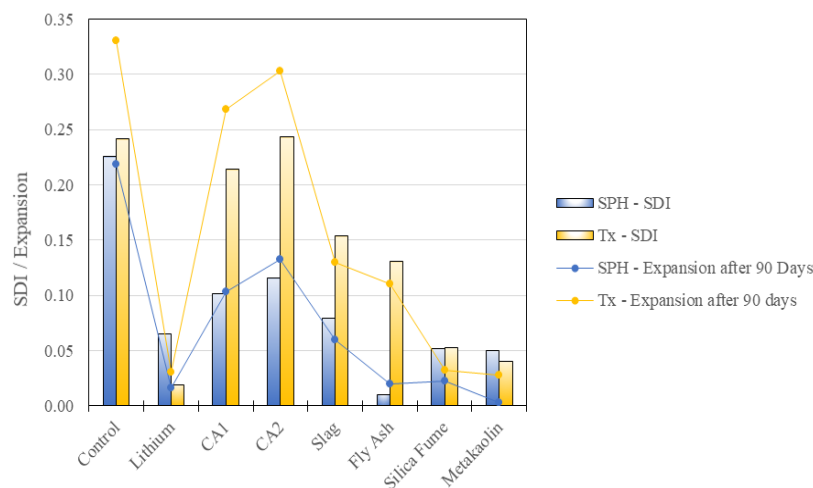


Figure 4.3: Stiffness damage indices for the ASR-affected concrete specimens.

4.3 Microscopy Assessment

Figure 4.4 presents the microscopic damage features and DRI numbers obtained from the ASR-affected concrete specimens. Globally, it is possible to see that all the DRI numbers obtained for the different mixtures and aggregate types increase as a function of the specimens' expansions. Greater DRI numbers were found in control specimens (912 for Tx Control and 723 for SPH Control) and followed by CA2 and CA1. The data obtained with the DRI are in agreement with the shear strength, modulus of elasticity and SDI results. Furthermore, the samples SF and MK, and, those with lithium-based systems obtained the lowest values, ranging between 137 and 160 on DRI numbers. Considering the aggregate's type (i.e. fine vs coarse aggregate), the results obtained were quite close; however, it is clear that the incorporation of Tx leads to a higher density of cracks in the cement paste.

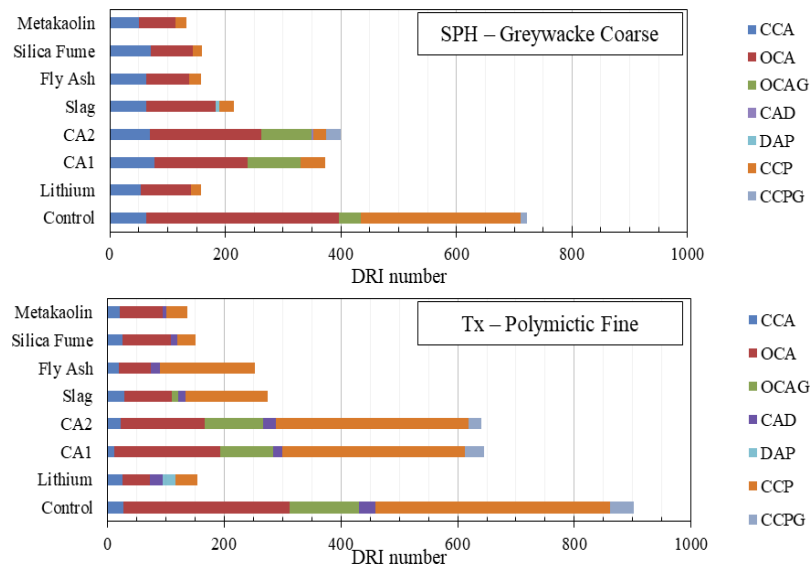


Figure 4.4: Damage Rating Index for the ASR-affected concrete specimens.

Besides the enhancement of the microstructure due to the natural healing process, the propagation of cracks due to ASR development was clearly modified by the artificial healing process generated by CA. As discussed in the literature [2,8,9,40], in affected samples at low expansion levels (e.g. 0.05-0.07%), cracks can be mainly found inside the aggregate particles and it is unlikely to find cracks in the cement paste extending from the aggregates. Moreover, until the point that the internal crack of the aggregates reaches the cement paste, it is unlike that CA admixtures start healing those cracks. In other words, a minimum influence on ASR-induced kinetics is observed. However, at moderate expansion levels (e.g. 0.10-0.12%), the cracks keep growing within the aggregates (in length and width), and extend to the cement paste. Therefore, crystalline admixtures (CA1 and CA2) can start healing the formed cracks in the cement paste, which may be responsible for the changes in the kinetics observed in Figure 4.1. Otherwise, the same behaviour is not seen for Tx reactive fine aggregates. This can be explained by the faster kinetics and crack development of this highly reactive aggregate, which does not give enough time for the healing process to take place.

The use of SCMs changes the microstructure of the matrix, interfering in the porosity of the hydrated cement paste and also, in the pores sizes, distribution and interconnectivity [53]. Regardless of the SCM's type (cementing or pozzolanic), besides the physical effect on the cement matrix, they also are able to form more C-S-H particles, decreasing the amount of portlandite in the pore solution, along with the pH. The use of SCMs in combination with CA1 was able to significantly change ASR-induced kinetics and damage. The CaO/SiO₂ ratio of the binder composition, which changes accordingly with the chemical composition of each SCM, is one of the most important parameters to be selected to suppress ASR. The most reactive SCMs used (i.e. Silica Fume and Metakaolin) were able to consume a significant amount of portlandite during their pozzolanic reactivity, changing the viscosity and swelling properties of the ASR-gel and, also, reducing the pH of the material. Moreover, the use of metakaolin shows that aluminum seems to play an important role to mitigate ASR; the presence of aluminum in the pore solution leads to a slower SiO₂ dissolution and reaction products formation when compared to control mixes [27].

5. CONCLUSIONS

The primary objective of this research program was to evaluate different concrete mixes presenting two different types of reactive aggregates (i.e. Greywacke Coarse and Polymictic Fine aggregates), incorporating a wide range of binder compositions (i.e. GU cement, metakaolin, silica fume, fly ash and slag) and using different types of admixtures (i.e. crystalline, water repellent and lithium-based products). From the results obtained in this study (up to 3 months of exposure), the following conclusions may be drawn:

- At least for the time-based evaluations, it seems that ASR kinetics, mechanical properties and microscopic changes are dependent on the aggregate's type (i.e. fine vs coarse aggregate).

Samples incorporating the highly reactive Tx sand were more damaged after 90 days of curing than SPH samples. Moreover, samples containing Tx have developed more cracks in the cement paste in shorter periods of time due to their faster ASR-induced kinetics;

- The use of crystalline admixtures (CA) was able to change the kinetics and distress caused by ASR, for both reactive aggregates used. It is believed that the CAs can start healing ASR deterioration only when the cracks reach the cement paste. This interesting behaviour can be drawn due to the significative change on ASR-induced kinetics of SPH mixtures after the point where cracks are expected to reach the cement paste;
- The combined use of different types of SCMs and crystalline admixtures was highly effective to mitigate ASR. However, the chemical composition of the SCMs plays an important role in the data collected;
- The use of Silica Fume and Metakaolin in combination with crystalline admixtures has yielded the best results so far, even better than the samples containing Lithium in the proportion of 0.74 Li/Na. Moreover, it has been found that the use of Metakaolin that presents an important amount of aluminum, seems to play an important role to mitigate ASR, since it leads to a slower SiO₂ dissolution;
- This research is current in progress. Different and more interesting and conclusive results will be obtained along the next months. Yet, up to date, it is clear that the combination of SCMs and crystalline admixtures are promising to mitigate ASR-induced development.

6. ACKNOWLEDGEMENTS

The authors would like to thank Dr. Muslim Majeed and Dr. Gamal Elnabelsya from the Materials and Structures Laboratory at the University of Ottawa. D. J. De Souza benefits from a Vanier scholarship financed by NSERC (Natural Sciences and Engineering Research Council of Canada).

7. REFERENCES

- [1] J. Lindgård, Ö. Andiç-Çakir, I. Fernandes, T.F. Rønning, M.D.A. Thomas, Alkali-silica reactions (ASR): Literature review on parameters influencing laboratory performance testing, *Cem. Concr. Res.* 42 (2012) 223–243. doi:10.1016/j.cemconres.2011.10.004.
- [2] M. Rashidi, M.C.L. Knapp, A. Hashemi, J.Y. Kim, K.M. Donnell, R. Zoughi, L.J. Jacobs, K.E. Kurtis, Detecting alkali-silica reaction: A multi-physics approach, *Cem. Concr. Compos.* 73 (2016) 123–135. doi:10.1016/j.cemconcomp.2016.07.001.
- [3] L.F.M. Sanchez, Contribution to the assessment of damage in aging concrete infrastructures affected by alkali-aggregate reaction, (2014) 341.
- [4] L.F.M. Sanchez, B. Fournier, M. Jolin, D. Mitchell, J. Bastien, Overall assessment of Alkali-Aggregate Reaction (AAR) in concretes presenting different strengths and incorporating a wide range of reactive aggregate types and natures, *Cem. Concr. Res.* 93 (2017) 17–31. doi:10.1016/j.cemconres.2016.12.001.
- [5] B. Fournier, M.-A. Bérubé, Alkali-aggregate reaction in concrete: a review of basic concepts and engineering implications, *Can. J. Civ. Eng.* 27 (2000) 167–191. doi:10.1139/cjce-27-2-167.
- [6] L. Sanchez, Contribution to the assessment of damage in aging concrete infrastructures affected by alkali-aggregate reaction, UNIVERSITE LAVAL, 2014.
- [7] L.F.M. Sanchez, B. Fournier, M. Jolin, J. Duchesne, Reliable quantification of AAR damage through assessment of the Damage Rating Index (DRI), *Cem. Concr. Res.* 67 (2015) 74–92. doi:10.1016/j.cemconres.2014.08.002.
- [8] L.F.M. Sanchez, B. Fournier, M. Jolin, J. Bastien, Evaluation of the stiffness damage test (SDT) as a tool for assessing damage in concrete due to ASR: Test loading and output responses for concretes incorporating fine or coarse reactive aggregates, *Cem. Concr. Res.* 56 (2014) 213–229. doi:10.1016/j.cemconres.2013.11.003.
- [9] L.F.M. Sanchez, B. Fournier, M. Jolin, M.A.B. Bedoya, J. Bastien, J. Duchesne, Use of Damage Rating Index to quantify alkali-silica reaction damage in concrete: Fine versus coarse aggregate, *ACI Mater. J.* 113 (2016) 395–407. doi:10.14359/51688983.

- [10] L.F.M. Sanchez, B. Fournier, M. Jolin, J. Bastien, D. Mitchell, Practical use of the Stiffness Damage Test (SDT) for assessing damage in concrete infrastructure affected by alkali-silica reaction, *Constr. Build. Mater.* 125 (2016) 1178–1188. doi:10.1016/j.conbuildmat.2016.08.101.
- [11] D.J. De Souza, L.F.M. Sanchez, M.T. De Grazia, Evaluation of a direct shear test setup to quantify AAR-induced expansion and damage in concrete, *Constr. Build. Mater.* 229 (2019). doi:10.1016/j.conbuildmat.2019.116806.
- [12] J. Duchesne, M.A. Bérubé, Long-term effectiveness of supplementary cementing materials against alkali-silica reaction, *Cem. Concr. Res.* 31 (2001) 1057–1063. doi:10.1016/S0008-8846(01)00538-5.
- [13] M. Thomas, The effect of supplementary cementing materials on alkali-silica reaction: A review, *Cem. Concr. Res.* 41 (2011) 1224–1231. doi:10.1016/j.cemconres.2010.11.003.
- [14] P. Shen, L. Lu, W. Chen, F. Wang, S. Hu, Efficiency of metakaolin in steam cured high strength concrete, *Constr. Build. Mater.* 152 (2017) 357–366. doi:10.1016/j.conbuildmat.2017.07.006.
- [15] J. Duchesne, M.-A. Bérubé, The Effectiveness Of Supplementary Cementing Materials In Suppressing Expansion Due To Asr: Another Look At The Reaction Mechanisms Part 1: Concrete Expansion And Portland'ie Depletion, *Cem. Concr. Res.* 24 (1994) 221–230.
- [16] Y. Kawabata, K. Yamada, The mechanism of limited inhibition by fly ash on expansion due to alkali-silica reaction at the pessimum proportion, *Cem. Concr. Res.* 92 (2017) 1–15. doi:10.1016/j.cemconres.2016.11.002.
- [17] Z. Shi, C. Shi, J. Zhang, S. Wan, Z. Zhang, Z. Ou, Alkali-silica reaction in waterglass-activated slag mortars incorporating fly ash and metakaolin, *Cem. Concr. Res.* 108 (2018) 10–19. doi:10.1016/j.cemconres.2018.03.002.
- [18] A.K. Saha, M.N.N. Khan, P.K. Sarker, F.A. Shaikh, A. Pramanik, The ASR mechanism of reactive aggregates in concrete and its mitigation by fly ash: A critical review, *Constr. Build. Mater.* 171 (2018) 743–758. doi:10.1016/j.conbuildmat.2018.03.183.
- [19] M.C.G. Juenger, R. Siddique, Recent advances in understanding the role of supplementary cementing materials in concrete, *Cem. Concr. Res.* (2015). doi:10.1016/j.cemconres.2015.03.018.
- [20] D. Hester, C. McNally, M. Richardson, A study of the influence of slag alkali level on the alkali-silica reactivity of slag concrete, *Constr. Build. Mater.* 19 (2005) 661–665. doi:10.1016/j.conbuildmat.2005.02.016.
- [21] T. Nochaiya, W. Wongkeo, A. Chaipanich, Utilization of fly ash with silica fume and properties of Portland cement-fly ash-silica fume concrete, *Fuel.* 89 (2010) 768–774. doi:10.1016/j.fuel.2009.10.003.
- [22] M.H. Shehata, M.D.A. Thomas, Use of ternary blends containing silica fume and fly ash to suppress expansion due to alkali-silica reaction in concrete, *Cem. Concr. Res.* 32 (2002) 341–349. doi:10.1016/S0008-8846(01)00680-9.
- [23] M.C.G. Juenger, C.P. Ostertag, Alkali-silica reactivity of large silica fume-derived particles, *Cem. Concr. Res.* 34 (2004) 1389–1402. doi:10.1016/j.cemconres.2004.01.001.
- [24] M. Rostami, K. Behfarnia, The effect of silica fume on durability of alkali activated slag concrete, *Constr. Build. Mater.* 134 (2017) 262–268. doi:10.1016/j.conbuildmat.2016.12.072.
- [25] A.M. Boddy, R.D. Hooton, M.D.A. Thomas, The effect of the silica content of silica fume on its ability to control alkali-silica reaction, *Cem. Concr. Res.* 33 (2003) 1263–1268. doi:10.1016/S0008-8846(03)00058-9.
- [26] J. Wei, B. Gencturk, A. Jain, M. Hanifehzadeh, Mitigating alkali-silica reaction induced concrete degradation through cement substitution by metakaolin and bentonite, *Appl. Clay Sci.* 182 (2019) 105257. doi:10.1016/j.clay.2019.105257.
- [27] A. Leemann, L. Bernard, S. Alahrache, F. Winnefeld, ASR prevention - Effect of aluminum and lithium ions on the reaction products, *Cem. Concr. Res.* 76 (2015) 192–201. doi:10.1016/j.cemconres.2015.06.002.

- [28] T. Kim, J. Olek, The effects of lithium ions on chemical sequence of alkali-silica reaction, *Cem. Concr. Res.* 79 (2016) 159–168. doi:10.1016/j.cemconres.2015.09.013.
- [29] C. Tremblay, M.A. Bérubé, B. Fournier, M.D. Thomas, K.J. Folliard, Experimental investigation of the mechanisms by which LiNO₃ is effective against ASR, *Cem. Concr. Res.* 40 (2010) 583–597. doi:10.1016/j.cemconres.2009.09.022.
- [30] X. Feng, M.D.A. Thomas, T.W. Bremner, B.J. Balcom, K.J. Folliard, Studies on lithium salts to mitigate ASR-induced expansion in new concrete: A critical review, *Cem. Concr. Res.* 35 (2005) 1789–1796. doi:10.1016/j.cemconres.2004.10.013.
- [31] X. Feng, M.D.A. Thomas, T.W. Bremner, K.J. Folliard, B. Fournier, New observations on the mechanism of lithium nitrate against alkali silica reaction (ASR), *Cem. Concr. Res.* 40 (2010) 94–101. doi:10.1016/j.cemconres.2009.07.017.
- [32] M. Cyr, P. Lawrence, E. Ringot, Mineral admixtures in mortars: Quantification of the physical effects of inert materials on short-term hydration, *Cem. Concr. Res.* 35 (2005) 719–730. doi:10.1016/j.cemconres.2004.05.030.
- [33] B. Lothenbach, K. Scrivener, R.D. Hooton, Supplementary cementing materials, *Cem. Concr. Res.* 41 (2011) 1244–1256. doi:10.1016/j.cemconres.2010.12.001.
- [34] X. Hou, L.J. Struble, R.J. Kirkpatrick, Formation of ASR gel and the roles of C-S-H and portlandite, *Cem. Concr. Res.* 34 (2004) 1683–1696. doi:10.1016/j.cemconres.2004.03.026.
- [35] X. Mo, Laboratory study of LiOH in inhibiting alkali-silica reaction at 20 °c: A contribution, *Cem. Concr. Res.* 35 (2005) 499–504. doi:10.1016/j.cemconres.2004.06.003.
- [36] M. Kawamura, H. Fuwa, Effects of lithium salts on ASR gel composition and expansion of mortars, *Cem. Concr. Res.* 33 (2003) 913–919. doi:10.1016/S0008-8846(02)01092-X.
- [37] D. Bulteel, E. Garcia-Diaz, P. Dégrugilliers, Influence of lithium hydroxide on alkali-silica reaction, *Cem. Concr. Res.* 40 (2010) 526–530. doi:10.1016/j.cemconres.2009.08.019.
- [38] A. Leemann, G. Le Saout, F. Winnefeld, D. Rentsch, B. Lothenbach, Alkali-Silica reaction: The Influence of calcium on silica dissolution and the formation of reaction products, *J. Am. Ceram. Soc.* 94 (2011) 1243–1249. doi:10.1111/j.1551-2916.2010.04202.x.
- [39] K. Sisomphon, O. Copuroglu, E.A.B. Koenders, Self-healing of surface cracks in mortars with expansive additive and crystalline additive, *Cem. Concr. Compos.* 34 (2012) 566–574. doi:10.1016/j.cemconcomp.2012.01.005.
- [40] K. Sisomphon, O. Copuroglu, E.A.B. Koenders, Effect of exposure conditions on self healing behavior of strain hardening cementing composites incorporating various cementing materials, *Constr. Build. Mater.* 42 (2013) 217–224. doi:10.1016/j.conbuildmat.2013.01.012.
- [41] L. Ferrara, V. Krelani, M. Carsana, A “fracture testing” based approach to assess crack healing of concrete with and without crystalline admixtures, *Constr. Build. Mater.* 68 (2014) 535–551. doi:10.1016/j.conbuildmat.2014.07.008.
- [42] H. Ma, S. Qian, Z. Zhang, Effect of self-healing on water permeability and mechanical property of Medium-Early-Strength Engineered Cementing Composites, *Constr. Build. Mater.* 68 (2014) 92–101. doi:10.1016/j.conbuildmat.2014.05.065.
- [43] C.M. Dry, Three designs for the internal release of sealants, adhesives, and waterproofing chemicals into concrete to reduce permeability, *Cem. Concr. Res.* 30 (2000) 1969–1977. doi:10.1016/S0008-8846(00)00415-4.
- [44] L.L. Kan, H.S. Shi, A.R. Sakulich, V.C. Li, Self-healing characterization of engineered cementing composite materials, *ACI Mater. J.* 107 (2010) 617–624. doi:10.14359/51664049.
- [45] P. Azarsa, R. Gupta, A. Biparva, Assessment of self-healing and durability parameters of concretes incorporating crystalline admixtures and Portland Limestone Cement, *Cem. Concr. Compos.* 99 (2019) 17–31. doi:10.1016/j.cemconcomp.2019.02.017.

- [46] L.F.M. Sanchez, B. Fournier, M. Jolin, J. Bastien, Evaluation of the Stiffness Damage Test (SDT) as a tool for assessing damage in concrete due to alkali-silica reaction (ASR): Input parameters and variability of the test responses, *Constr. Build. Mater.* 77 (2015) 20–32. doi:10.1016/j.conbuildmat.2014.11.071.
- [47] L.F.M. Sanchez, T. Drimalas, B. Fournier, D. Mitchell, J. Bastien, Comprehensive damage assessment in concrete affected by different internal swelling reaction (ISR) mechanisms, *Cem. Concr. Res.* 107 (2018) 284–303. doi:10.1016/j.cemconres.2018.02.017.
- [48] B. Barr, E.B.D. Hasso, Development of a compact cylindrical shear test specimen, *J. Mater. Sci. Lett.* 5 (1986) 1305–1308.
- [49] R.S. Crouch, J.G.M. Wood, Damage evolution in AAR affected concretes, *Eng. Fract. Mech.* 35 (1990) 211–218. doi:10.1016/0013-7944(90)90199-Q.
- [50] S. Dean, N. Smaoui, B. Bissonnette, M. Bérubé, B. Fournier, B. Durand, Mechanical Properties of ASR-Affected Concrete Containing Fine or Coarse Reactive Aggregates, *J. ASTM Int.* 3 (2006) 12010. doi:10.1520/JAI12010.
- [51] N. Smaoui, B. Bissonnette, M. Bérubé, B. Fournier, B. Durand, Mechanical Properties of ASR-Affected Concrete Containing Fine or Coarse Reactive Aggregates, *J. ASTM Int.* 3 (2006) 12010. doi:10.1520/JAI12010.
- [52] D.J. De Souza, L. Sanchez, F. Ahimoghadam, G. Fathifazl, Comparison Among Different Mix-Design Procedures for RCA Concrete, *ACI Spec. Publ. SP-334* (2019) 99–121. <https://www.concrete.org/publications/internationalconcreteabstractsportal.aspx?m=details&ID=51720255>.
- [53] D.J. Souza, L.Y. Yamashita, F. Dranka, M.H.F. Medeiros, R.A. Medeiros-Junior, Repair Mortars Incorporating Multiwalled Carbon Nanotubes: Shrinkage and Sodium Sulfate Attack, *J. Mater. Civ. Eng.* 29 (2017) 1–12. doi:10.1061/(ASCE)MT.1943-5533.0002105.